American Mineralogist, Volume 76, pages 1380–1388, 1991

Crystal chemistry of Fe- and Cr-rich warwickite

SIMONA BIGI, MARIA FRANCA BRIGATTI, SILVIO CAPEDRI
Istituto di Mineralogia e Petrografia, Università di Modena, Via S. Eufemia 19, 41100 Modena, Italy

ABSTRACT

Warwickite is an orthorhombic oxyborate mineral with the general formula $^{[6]}M_2O^{[3]}BO_3$ ($M = Mg^{2+}$, Mn^{2+}, Fe^{3+}, Ti^{4+}, Al^{3+}). The studied warwickite samples are from lamproitic rocks (jumillites) and associated carbonatite-like veins (Jumilla, Murcia province, southeast Spain). Their chemical compositions are quite variable and different from those of warwickite described in the literature: in particular, Cr_2O_3 varies between 0.0 and 13.5 wt%, total wt% Fe as Fe_2O_3 is as high as 50.6 wt% and total wt% TiO_2 as high as 10.2 wt%. Two main substitutions occur in Jumilla warwickite: $Mg^{2+} + Ti^{4+} \rightleftharpoons 2Fe^{3+}$ and $Fe^{3+} \rightleftharpoons Cr^{3+}$.

The structures of seven crystals of different compositions were refined in space group *Pnma*, giving $R = 0.018$–0.038. The structural results show that: (1) The M1 octahedron is smaller and more distorted than the M2 octahedron. (2) Distortion of the octahedral layer is greater in Fe-rich warwickite. (3) Fe preferentially enters the M1 site. (4) The M2-O4 distance decreases with increasing Ti, suggesting preferential ordering at the M2 site. TEM studies show planar (100) defects. These defects cause variations in the octahedral chain length.

INTRODUCTION

The name warwickite is applied to an unusual family of orthorhombic oxyborate minerals (space group *Pnma*; $a \simeq 9.20$, $b \simeq 3.09$, $c \simeq 9.36$ Å) of ideal composition $^{[6]}M_2O^{[3]}BO_3$ ($M = Mg^{2+}$, Mn^{2+}, Fe^{3+}, Ti^{4+}, Al^{3+}). The structure was first investigated by Takéuchi et al. (1950) for warwickite of composition $(Mg,Fe)_{1.5}Ti_{0.5}OBO_3$. Compositions of other warwickite structures refined subsequently include $Mg_{1.33}Al_{0.21}Fe_{0.12}Ti_{0.34}OBO_3$ (Moore and Araki, 1974) and the synthetic compounds $FeCoOBO_3$ (Venkatakrishnan and Buerger, 1972) and $MgScOBO_3$ and $Mg_{0.76}Mn_{1.24}OBO_3$ (Norrestam, 1989).

According to Hawthorne (1986), warwickite belongs to a subgroup of the infinite framework $^{[6]}M_x^{[3]}T_y\Phi_z$ minerals, characterized by chains of edge-sharing octahedra ($^{[6]}M_2$) with a repeat distance that is an integral multiple of 3 Å. The chains, canted at 60° to each other, are cross linked by $(BO_3)^{3-}$ triangles in the plane perpendicular to the length of the chain and by sharing edges to form ribbons four octahedra wide (Fig. 1). These geometrical features are common to other mineral groups; thus, Merlino and Perchiazzi (1988) proposed structural analogies between oxyborates and the minerals of the cuspidine family, in which two parallel $(BO_3)^{3-}$ groups are replaced by one $(Si_2O_7)^{6-}$ group. Moore and Araki (1974) consider warwickite a member of the structural group denoted as "3 Å wallpaper structures" because of the two-dimensional character and the short length of the *c*-axis (if the mineral is referred to the nonstandard space group *Pnam*). According to Norrestam (1989), the ratio of divalent to trivalent cations is 1:3 and 3:1 at the M1 and M2 sites, respectively, for $MgScOBO_3$ (*Pnam*) and $Mg_{0.76}Mn_{1.24}OBO_3$ ($P2_1/a$).

Natural occurrences of warwickite are rare; they have been described in marbles from Edenville (Takéuchi et al., 1950) and from Amity (Moore and Araki, 1974), both in the town of Warwick (Orange County, New York), and from Taigs (Southern Yakutia, U.S.S.R.) (Malinko et al., 1986).

Warwickite samples from the lamproites of Jumilla (Murcia province, southeast Spain) are compositionally unlike those previously described; they are rich in Fe (Fe_2O_3 up to 50.6 wt%) and contain significant Cr (Cr_2O_3 up to 13.5 wt%). As the composition of Jumilla samples varies widely, they are suitable for examination of the structural changes associated with variation in composition.

OCCURRENCE OF WARWICKITE AND PETROGRAPHIC FEATURES OF THE HOST ROCKS

Lamproitic rocks (7.2–7.6 Ma; Nobel et al., 1981) constitute two outcrops near La Celia, about 13 km west of Jumilla (Fig. 2). The smaller outcrop is composed of porphyritic lavas only, whereas the larger outcrop contains porphyritic and coarser-grained subvolcanic rocks as well as genetically related carbonatite-like rocks (Venturelli et al., 1991). The lamproitic rocks (jumillites as defined by Osann, 1906) have been extensively studied (e.g., Fuster et al., 1967; Venturelli et al., 1984). They are composed mainly of phlogopite, olivine, apatite, and occasional clinopyroxene as phenocrysts, whereas the groundmass is composed of the same phases together with sanidine or

0003–004X/91/0708–1380$02.00

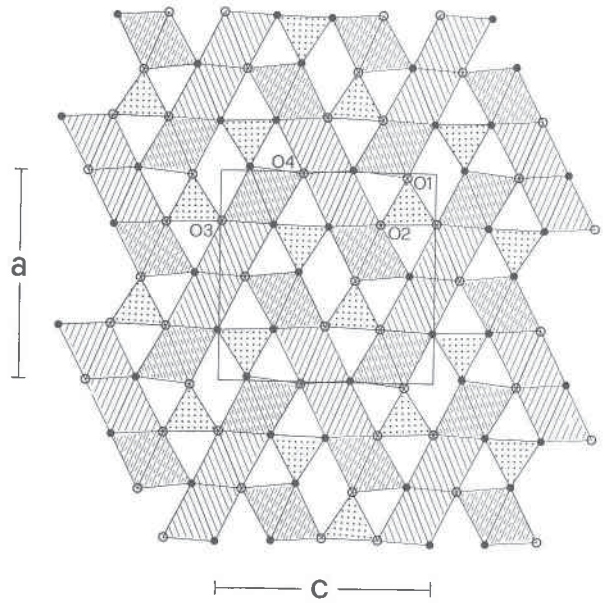

Fig. 1. Polyhedral representation of the warwickite structure viewed down **b**. Ruled octahedra = M1; dashed octahedra = M2; stippled triangles = B; O atoms at $y = ¼$ are black circles; O atoms at $y = ¾, -¼$ are open circles.

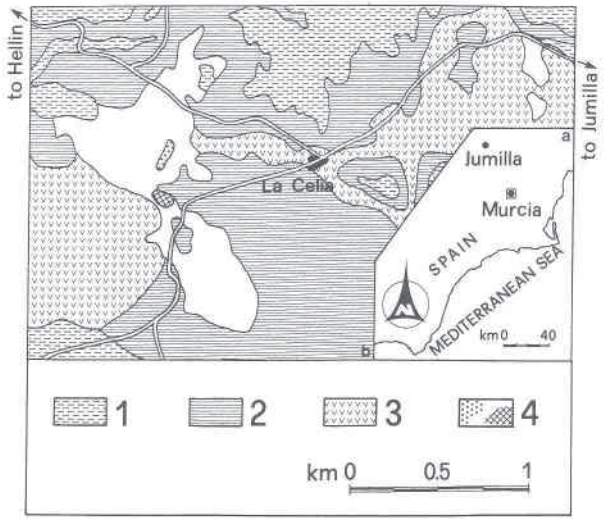

Fig. 2. Sketch map of the geological relations in the area of the Jumilla lamproite. 1 = Quaternary continental sediments; 2 = Miocenic continental sediments; 3 = Triassic evaporites; 4 = jumillites. The dotted area refers to the carbonatite-like outcrop where the warwickite occurs (Venturelli, personal communication).

analcime, K-rich richterite, subordinate carbonates, and accessory pseudobrookite, ilmenite, magnetite, and warwickite. Brown glass is occasionally present in the groundmass. In the subvolcanic rocks, the groundmass is composed mainly of sanidine oikocrysts (up to 5 mm) containing phlogopite, olivine, clinopyroxene, analcime, pseudobrookite, and opaques. The interstices defined by the large sanidine crystals are filled either with richterite, analcime, phlogopite, sanidine, oxides, and glass or with magmatic carbonates and Na-rich clinopyroxene, phlogopite, sanidine, potassium amphibole, apatite, pseudobrookite, hematite, and warwickite.

Carbonatite-like veins permeate lamproites in a small area (150 m long, 40 m wide) in the larger outcrop. The carbonatite-like rocks probably crystallized in the range 700–600 °C and under high f_{O_2} (≥HM buffer). They are composed mainly of granular calcite (with subordinate globular dolomite that replaces calcite) with fluorapatite, hematite-ferrian ilmenite crystals, subordinate Na-rich clinopyroxene, phlogopite, sanidine, pseudobrookite, very rare zircon, and quartz. Warwickite is frequently an accessory phase and occasionally a main phase. This is the case for a carbonatite-like veinlet (1 cm across) which may be seen along the pathway cut into the lamproites leading to the southern entrance of the old hematite quarry, the location of most of the warwickites reported here. Warwickite constitutes about 10% by volume and is concentrated along the walls of the veinlet in sheaflike aggregates of black shiny prismatic crystals (0.6 mm long with square cross section) extending toward the center of the vein. The luster is pearly to adamantine. The crystals are brittle and show good {010} cleavage. In thin section, they are deep yellow to light brown and show slight pleochroism with maximum absorption parallel to the length; they are uniaxial positive.

Experimental techniques

Chemical analyses

Warwickite samples were analyzed (Tables 1 and 2) using an ARL-SEMQ electron microprobe at the Istituto di Mineralogia e Petrografia, Università di Modena. The wavelength-dispersive method was used, operating at 15 kV accelerating voltage, 20 nA sample current, 3 μm beam diameter, and 20 s counting time on peak and 2 s on backgrounds. Natural minerals were used as standards; the data were reduced by the method of Ziebold and Ogilvie (1964) using the correction factors of Albee and Ray (1970). B could not be determined quantitatively on single crystals; it was qualitatively analyzed by atomic absorption on concentrates of warwickite. Warwickite, both in polished thin sections and as crystals used for structure refinement, was analyzed. Average chemical compositions of homogeneous grains and selected representative analyses obtained on zoned crystals are reported in Table 1. The crystals used for structural refinement are chemically homogeneous, and their compositions (averaged from 6 to 10 analyses per grain) are reported in Table 2.

The chemical formulas reported in Tables 1 and 2 have been obtained, starting from the general formula $^{[6]}M_8{}^{[3]}T_4O_{16}$ (Hawthorne, 1986). Only those analyses for which the total octahedral content ($^{[6]}\Sigma$) was in the range 7.99–8.01 apfu (atoms per formula unit) were used for further investigation. All Fe was calculated as Fe^{3+} as suggested by the high oxidizing conditions of the carbon-

TABLE 1. Representative electron-microprobe analyses and chemical formulae on the basis of $M_8O_4T_4O_{12}$ of warwickite from Jumilla lamproites

	1	2	3	4	5	6	7	8	9	10	11	12	13	14	15	16	17	18	19	20	21	22
MgO	32.11	30.37	30.91	31.82	31.81	30.64	31.11	32.10	31.34	32.18	30.85	33.20	32.86	30.54	29.36	31.60	32.81	26.49	27.59	29.23	32.23	28.52
CaO	0.11	0.07	0.10	0.16	0.10	0.32	0.37	0.09	0.06	0.07	0.10	0.04	0.02	0.14	0.05	0.15	0.08	0.10	0.07	0.07	0.03	0.01
MnO	0.12	0.13	0.26	0.28	0.23	0.34	0.36	0.15	0.11	0.18	0.17	0.14	0.19	0.12	0.26	0.08	0.07	0.28	0.07	0.12	0.14	0.22
Al_2O_3	0.29	0.19	0.31	0.38	0.40	0.35	0.33	0.27	0.27	0.32	0.35	0.35	—	—	0.49	0.30	0.37	0.04	0.16	0.33	0.28	0.42
Cr_2O_3	0.93	0.81	0.96	0.78	0.61	0.41	0.81	11.65	11.55	9.75	11.99	9.32	9.64	12.93	7.82	10.11	9.14	0.67	0.78	11.05	10.81	12.62
Fe_2O_3	33.57	38.95	36.22	33.68	34.34	36.83	35.17	23.54	25.00	24.55	25.64	22.60	23.41	26.49	33.85	25.90	24.11	48.94	46.50	32.00	23.64	32.05
TiO_2	9.15	5.97	7.83	9.07	8.48	7.37	8.02	8.00	7.96	8.93	6.99	10.15	9.94	6.16	4.53	7.79	9.10	0.79	1.72	3.55	8.76	2.75
ZrO_2	—	—	—	0.20	0.20	0.11	0.11	0.01	—	0.12	0.03	0.02	—	—	0.03	—	0.16	—	0.08	—	0.05	0.05
Nb_2O_5	—	—	—	—	0.20	0.18	0.13	0.21	0.14	0.10	0.15	0.11	—	—	0.24	0.22	0.16	0.06	0.08	0.28	0.14	0.24
B_2O_3	23.42	22.72	23.25	23.41	23.32	23.12	23.44	23.22	23.34	23.36	23.01	23.44	23.44	23.12	22.77	23.29	23.28	22.32	22.28	22.67	23.21	22.92
SiO_2	0.30	0.79	0.16	0.21	0.31	0.32	0.13	0.76	0.23	0.43	0.71	0.63	0.49	0.49	0.59	0.56	0.71	0.30	0.67	0.71	0.70	0.21
Mg	4.71	4.53	4.57	4.68	4.68	4.54	4.59	4.70	4.61	4.71	4.55	4.82	4.79	4.52	4.39	4.64	4.79	4.06	4.20	4.38	4.72	4.28
Ca	0.01	0.01	0.01	0.02	0.01	0.03	0.04	0.01	0.01	0.01	0.01	—	—	0.01	0.01	0.02	0.01	0.02	0.01	0.01	—	—
Mn	0.01	0.01	0.02	0.02	0.02	0.03	0.03	0.01	0.01	0.02	0.01	0.01	0.02	0.01	0.02	0.01	0.01	0.02	0.01	0.01	0.01	0.02
Al	0.03	0.02	0.04	0.04	0.05	0.04	0.04	0.03	0.03	0.04	0.04	0.04	—	—	0.06	0.04	0.04	—	0.02	0.04	0.03	0.05
Cr	0.07	0.06	0.08	0.06	0.05	0.03	0.06	0.91	0.90	0.76	0.94	0.72	0.75	1.02	0.62	0.79	0.71	0.05	0.06	0.88	0.84	1.01
Fe^{3+}	2.49	2.93	2.71	2.50	2.55	2.76	2.62	1.74	1.86	1.81	1.91	1.66	1.72	1.98	2.55	1.92	1.78	3.79	3.57	2.42	1.75	2.43
Ti	0.68	0.45	0.58	0.67	0.63	0.55	0.60	0.59	0.59	0.66	0.52	0.74	0.73	0.46	0.34	0.58	0.67	0.06	0.13	0.27	0.65	0.21
Zr	—	—	—	0.01	0.01	0.01	0.01	—	—	0.01	—	—	—	—	—	—	0.01	—	—	—	—	—
Nb	—	—	—	—	0.01	0.01	0.01	0.01	0.01	—	0.01	—	—	—	0.01	0.01	0.01	—	—	0.01	0.01	0.01
$^{[6]}\Sigma$	8.00	8.01	8.01	8.00	8.01	8.00	8.00	8.00	8.01	8.01	7.99	8.01	8.01	8.00	8.00	7.99	8.01	8.01	8.01	8.01	8.00	8.01
B	3.98	3.92	3.98	3.98	3.97	3.97	4.00	3.93	3.97	3.95	3.93	3.94	3.95	3.96	3.94	3.96	3.93	3.96	3.92	3.93	3.93	3.98
Si	0.03	0.08	0.02	0.02	0.03	0.03	0.01	0.07	0.02	0.04	0.07	0.06	0.05	0.05	0.06	0.05	0.07	0.03	0.07	0.07	0.07	0.02
$^{[3,4]}\Sigma$	4.01	4.00	3.99	4.00	4.00	4.00	4.02	4.01	3.99	4.00	4.00	4.00	4.00	4.01	4.00	4.01	4.00	3.99	3.99	4.00	4.00	4.00
O	16.00	16.00	16.00	16.00	16.00	16.00	16.00	16.00	16.00	16.00	16.00	16.00	16.00	16.00	16.00	16.00	16.00	16.00	16.00	16.00	16.00	16.00

	M1	M2	M3	M4	M5	M6
MgO	32.45 (32.24–32.65)	30.94 (29.59–32.16)	30.40 (27.44–32.63)	26.16 (25.68–26.61)	30.23 (28.78–31.22)	28.36 (26.58–29.95)
CaO	0.05 (0.02–0.07)	0.07 (0.05–0.09)	0.22 (0.15–0.32)	0.22 (0.18–0.24)	0.05 (0.03–0.06)	0.02 (0.00–0.04)
MnO	0.14 (0.13–0.15)	0.13 (0.12–0.15)	0.17 (0.08–0.31)	0.35 (0.19–0.61)	0.20 (0.07–0.42)	0.24 (0.10–0.52)
Al_2O_3	0.22 (0.19–0.23)	0.27 (0.26–0.28)	0.41 (0.32–0.71)	0.08 (0.03–0.19)	0.25 (0.21–0.28)	0.30 (0.25–0.35)
Cr_2O_3	10.27 (9.87–10.56)	10.45 (8.49–11.69)	8.59 (4.92–10.76)	0.23 (0.00–0.61)	11.66 (9.32–13.45)	6.78 (1.59–11.92)
Fe_2O_3	23.97 (23.10–24.78)	27.11 (25.79–29.70)	30.16 (23.63–41.20)	49.73 (48.73–50.63)	27.97 (26.51–29.55)	37.80 (28.94–47.07)
TiO_2	8.63 (7.85–9.13)	7.31 (5.15–9.03)	6.34 (1.85–9.82)	0.39 (0.21–0.62)	5.92 (4.39–8.34)	3.17 (1.02–5.85)
ZrO_2	0.18 (0.06–0.26)	0.03 (0.00–0.05)	0.06 (0.00–0.18)	0.10 (0.06–0.15)	0.05 (0.00–0.11)	0.04 (0.00–0.08)
Nb_2O_5	0.15 (0.14–0.17)	0.18 (0.13–0.23)	0.15 (0.11–0.19)	0.07 (0.03–0.12)	0.18 (0.11–0.23)	0.19 (0.11–0.28)
B_2O_3	23.21 (23.19–23.22)	23.22 (23.02–23.40)	23.05 (22.41–23.45)	22.24 (22.02–22.39)	23.01 (22.71–23.19)	22.72 (22.39–22.99)
SiO_2	0.71 (0.69–0.73)	0.30 (0.25–0.34)	0.47 (0.13–0.72)	0.43 (0.27–0.74)	0.50 (0.14–0.76)	0.37 (0.17–0.53)
Mg	4.75 (4.73–4.77)	4.57 (4.41–4.71)	4.50 (4.16–4.76)	4.02 (3.95–4.08)	4.48 (4.30–4.60)	4.27 (4.06–4.45)
Ca	0.01 (0.00–0.01)	0.01 (0.01–0.01)	0.03 (0.02–0.04)	0.02 (0.02–0.03)	0.01 (0.00–0.01)	0.00 (0.00–0.00)
Mn	0.01 (0.01–0.01)	0.01 (0.01–0.01)	0.02 (0.01–0.03)	0.03 (0.02–0.05)	0.02 (0.01–0.04)	0.02 (0.01–0.05)
Al	0.03 (0.02–0.03)	0.03 (0.03–0.03)	0.05 (0.03–0.08)	0.01 (0.00–0.02)	0.03 (0.02–0.03)	0.04 (0.03–0.04)
Cr	0.80 (0.77–0.82)	0.82 (0.66–0.92)	0.68 (0.40–0.85)	0.02 (0.00–0.05)	0.92 (0.73–1.07)	0.54 (0.13–0.94)
Fe^{3+}	1.77 (1.70–1.82)	2.02 (1.91–2.23)	2.26 (1.74–3.15)	3.86 (3.77–3.94)	2.10 (1.97–2.23)	2.88 (2.17–3.63)
Ti	0.64 (0.58–0.67)	0.54 (0.39–0.67)	0.47 (0.14–0.72)	0.03 (0.02–0.05)	0.44 (0.33–0.62)	0.24 (0.08–0.44)
Zr	0.01 (0.00–0.01)	0.00 (0.00–0.00)	0.00 (0.00–0.01)	0.01 (0.00–0.01)	0.00 (0.00–0.01)	0.00 (0.00–0.00)
Nb	0.01 (0.01–0.01)	0.01 (0.01–0.01)	0.01 (0.01–0.01)	0.00 (0.00–0.01)	0.01 (0.00–0.01)	0.01 (0.01–0.01)
$^{[6]}\Sigma$	8.01 (8.01–8.01)	8.00 (8.00–8.01)	8.01 (8.00–8.01)	8.00 (7.99–8.01)	8.00 (7.99–8.01)	8.00 (7.99–8.01)
B	3.93 (3.92–3.94)	3.96 (3.96–3.97)	3.95 (3.93–3.99)	3.95 (3.91–3.98)	3.95 (3.91–3.98)	3.96 (3.94–3.98)
Si	0.07 (0.07–0.07)	0.03 (0.03–0.03)	0.05 (0.01–0.07)	0.05 (0.03–0.08)	0.05 (0.01–0.08)	0.04 (0.02–0.05)
$^{[3,4]}\Sigma$	4.00 (3.99–4.01)	3.99 (3.99–4.01)	4.00 (3.99–4.00)	4.00 (3.99–4.01)	4.00 (3.99–4.02)	4.00 (3.99–4.00)
O	16.00 (16.00–16.00)	16.00 (16.00–16.00)	16.00 (16.00–16.00)	16.00 (16.00–16.00)	16.00 (16.00–16.00)	16.00 (16.00–16.00)

Note: The minimum and maximum range variation is reported in brackets for zoned crystals; samples 1 to 7 from jumillites, the remaining samples from carbonatite-like veins.

TABLE 2. Chemical compositions of the warwickite crystals used for structure refinement

	S1	S2	S3	S4	S5	S6	S7
MgO	28.26	30.82	31.43	32.58	31.31	32.35	30.02
CaO	—	0.06	—	—	0.03	0.04	0.04
MnO	0.05	0.14	0.05	0.05	0.11	0.03	0.04
Al_2O_3	0.94	0.36	1.19	0.55	0.21	0.79	0.52
Cr_2O_3	0.84	11.88	9.06	8.20	2.00	0.80	11.71
Fe_2O_3	44.48	26.21	27.54	25.57	34.58	33.00	28.91
TiO_2	2.02	6.62	6.64	8.96	8.05	9.16	5.09
ZrO_2	0.03	0.05	0.09	0.07	0.05	0.01	—
Nb_2O_5	0.06	0.25	—	—	0.11	0.02	0.10
B_2O_3	22.45	23.18	23.15	23.37	23.24	23.29	22.96
SiO_2	0.86	0.42	0.85	0.64	0.30	0.50	0.62
Mg	4.27	4.55	4.61	4.75	4.62	4.73	4.46
Ca	—	0.01	—	—	—	—	—
Mn	—	0.01	—	—	0.01	—	—
Al	0.11	0.04	0.14	0.06	0.02	0.09	0.06
Cr	0.07	0.93	0.71	0.63	0.16	0.06	0.92
Fe^{3+}	3.39	1.95	2.04	1.88	2.58	2.44	2.17
Ti	0.15	0.49	0.49	0.66	0.60	0.68	0.38
Zr	—	—	—	—	—	—	—
Nb	—	0.01	—	—	—	—	—
$^{[6]}\Sigma$	8.00	8.00	8.00	8.00	8.00	8.01	8.00
B	3.92	3.96	3.93	3.95	3.97	3.94	3.94
Si	0.09	0.04	0.08	0.06	0.03	0.05	0.06
$^{[3,4]}\Sigma$	4.01	4.00	4.01	4.01	4.00	3.99	4.00
O	16.00	16.00	16.00	16.00	16.00	16.00	16.00

Note: Sample S6 from jumillite; the remaining samples from carbonatite-like veins.

atite-like rocks and by the general indications of the structure refinement; Mn was assumed to be Mn^{2+}. Silica was assigned to tetrahedral coordination (for explanation, see the crystal chemistry section).

X-ray data collection and refinement

Seven chemically homogeneous warwickite crystals from the carbonatite-like vein were selected for the intensity data collection. Systematic absences are consistent with space group *Pnma*. The crystals were mounted on a CAD4 diffractometer operating at 52 kV and 40 mA with graphite-monocromated Mo$K\alpha$ X-radiation. Unit-cell parameters were obtained by least-squares refinement using 25 reflections $18° \leq \theta \leq 25°$ (Table 3). Starting from the results of an ω/θ plot based on ten selected reflections (Einstein, 1974), all intensities were measured using the ω-scan technique (scan width 0.8–1.8°). Background counts were made ±25% beyond the peak scan range. Three standard intensities and orientations were monitored every 2 h and 200 reflections, respectively; no significant deviation was noted during the data measurement.

The equivalent pairs (hkl) and ($\bar{h}kl$) were measured in the $2° < \theta < 33°$ range, k and l starting from zero. The resulting intensities were corrected for background, Lorentz-polarization, and absorption effects following the semiempirical method of North et al. (1968), and equivalent pairs were averaged (discrepancy factor R_{sym} = 0.013–0.041). A reflection was considered as observed if $I > 3\sigma I$.

Structure refinement was carried out using SHELX-76 (Sheldrick, 1976) and starting from the atomic coordinates and isotropic displacement factors of Moore and Araki (1974), modified for the difference in orientation (*Pnma*). Scattering and anomalous dispersion factors were taken from the *International Tables for X-ray Crystallography* (1974). Neutral B, half-ionized O, and fully ionized M cation scattering factors were used; as the scattering factors for Ti^{4+}, Fe^{3+}, and Cr^{3+} are similar, only Fe^{3+} and Mg^{2+} scattering curves were used at the M1 and M2 sites. The final difference-electron density map showed only random variations, with maxima between ±0.5 e/Å^3 and ±0.3 e/Å^3 for all samples. The atomic coordinates and displacement factors for the seven refined samples are listed in Table 4; Table 5 reports selected interatomic distances and Table 6,[1] the observed and calculated structure factors. Mean atomic numbers at the octahedral sites (estimated by structure refinement and by electron probe microanalysis) are listed in Table 7.

TEM study

Finely ground warwickite crystals were dispersed on holey carbon films supported on a Cu grid and coated lightly with C; they were examined with a Philips 400T transmission electron microscope operated at 100 keV with C_s = 2.8 mm and a resolving power of 4 Å. High-resolution images were obtained with underfocus condi-

[1] To obtain a copy of Table 6, order Document AM-91-465 from the Business Office, Mineralogical Society of America, 1130 Seventeenth Street NW, Suite 330, Washington, DC 20036, U.S.A. Please remit $5.00 in advance for the microfiche.

TABLE 3. Crystallographic data and parameters of the studied warwickite samples

Sample	Dimensions (mm)	$N_{uni.}$	$N_{obs.}$	$R_{sym.}$ ×100	$R_{obs.}$ ×100	a [Å]	b [Å]	c [Å]	V [Å^3]
S1	0.05 × 0.06 × 0.09	470	455	2.12	2.46	9.246(1)	3.0927(2)	9.384(1)	268.3
S2	0.02 × 0.03 × 0.15	349	348	3.06	1.88	9.226(2)	3.0860(7)	9.369(1)	266.8
S3	0.03 × 0.04 × 0.13	403	400	1.30	2.32	9.230(5)	3.0906(8)	9.378(3)	267.5
S4	0.02 × 0.02 × 0.13	328	328	2.23	1.87	9.228(1)	3.0840(5)	9.371(1)	266.7
S5	0.02 × 0.03 × 0.11	343	343	2.54	1.79	9.246(3)	3.0993(5)	9.378(2)	268.7
S6	0.01 × 0.01 × 0.06	288	268	4.07	3.84	9.242(4)	3.098(1)	9.383(1)	268.7
S7	0.03 × 0.04 × 0.08	432	430	2.40	2.63	9.255(1)	3.0941(8)	9.402(1)	269.3

Note: Samples as in Table 2; $R_{sym} = \frac{\sum_{hkl}\sum_{i=1}^{N} |I_{hkl_i} - I_{hkl}|}{\sum_{hkl}\sum_{i=1}^{N} I_{hkl}}$. Shown are crystal size, number of unique and observed reflections, agreement factors, and lattice parameters.

TABLE 4. Atom coordinates and equivalent isotropic and anisotropic displacement factors [Å²] for the studied warwickites

Atom	x	y	z	B_{eq}	β_{11}*	β_{22}*	β_{33}*	β_{13}*
Sample S1								
O1	0.0212(2)	0.25	0.8648(2)	1.03(5)	0.93(6)	1.02(7)	1.14(7)	−0.12(6)
O2	0.2469(2)	0.25	0.7465(2)	1.10(6)	1.10(7)	0.92(8)	1.28(8)	0.06(5)
O3	0.2387(2)	0.25	0.0064(2)	1.05(6)	0.96(6)	1.25(8)	0.95(7)	0.02(5)
O4	0.0091(2)	0.25	0.3870(2)	1.00(5)	0.90(6)	1.18(7)	0.93(6)	0.04(6)
M1	0.11564(5)	0.25	0.56885(5)	1.08(1)	1.17(2)	1.02(2)	1.04(2)	−0.08(2)
M2	0.10278(7)	0.25	0.18992(6)	1.19(2)	1.12(3)	1.17(3)	1.29(3)	0.03(2)
B	0.1678(3)	0.25	0.8741(3)	0.90(7)	0.75(8)	0.9(1)	1.02(9)	0.06(9)
Sample S2								
O1	0.0202(2)	0.25	0.8680(3)	1.39(6)	1.46(7)	1.50(8)	1.21(8)	−0.36(8)
O2	0.2463(2)	0.25	0.7469(2)	1.29(7)	1.36(8)	1.3(1)	1.21(9)	0.20(6)
O3	0.2386(2)	0.25	0.0057(2)	1.35(7)	1.41(8)	1.8(1)	0.81(9)	−0.34(6)
O4	0.0098(2)	0.25	0.3841(3)	1.21(6)	1.44(7)	1.26(8)	0.93(7)	0.05(7)
M1	0.11569(6)	0.25	0.56890(6)	1.27(2)	1.58(2)	1.04(2)	1.19(2)	−0.06(2)
M2	0.10218(9)	0.25	0.19020(7)	1.17(3)	1.41(3)	1.02(4)	1.07(4)	0.07(3)
B	0.1658(4)	0.25	0.8752(4)	1.5(1)	2.3(1)	1.6(1)	0.6(1)	0.2(1)
Sample S3								
O1	0.0208(2)	0.25	0.8674(3)	1.42(6)	1.58(8)	1.24(8)	1.44(9)	−0.24(8)
O2	0.2465(2)	0.25	0.7471(2)	1.38(7)	1.64(8)	1.3(1)	1.15(9)	0.24(7)
O3	0.2376(2)	0.25	0.0054(2)	1.29(7)	1.64(8)	1.11(9)	1.13(9)	−0.38(7)
O4	0.0101(2)	0.25	0.3835(3)	1.35(6)	1.80(8)	0.93(7)	1.31(8)	0.13(8)
M1	0.11567(6)	0.25	0.56875(6)	1.21(2)	1.66(2)	0.66(2)	1.31(2)	−0.05(2)
M2	0.10266(9)	0.25	0.19032(8)	1.13(3)	1.42(3)	0.60(3)	1.36(4)	0.00(3)
B	0.1674(4)	0.25	0.8750(4)	1.3(1)	1.9(1)	0.9(1)	1.1(1)	0.1(1)
Sample S4								
O1	0.0203(2)	0.25	0.8669(3)	1.37(7)	1.11(7)	1.88(9)	1.12(9)	−0.14(8)
O2	0.2468(2)	0.25	0.7475(2)	1.41(8)	1.39(9)	2.0(1)	0.8(1)	0.22(7)
O3	0.2388(2)	0.25	0.0053(2)	1.44(8)	1.42(9)	1.9(1)	1.0(1)	−0.28(7)
O4	0.0090(2)	0.25	0.3842(3)	1.26(7)	1.24(7)	1.40(9)	1.15(8)	0.18(8)
M1	0.11556(6)	0.25	0.56885(6)	1.16(2)	1.15(2)	1.15(3)	1.16(2)	−0.06(2)
M2	0.10245(9)	0.25	0.19035(8)	1.06(3)	1.02(3)	0.91(4)	1.25(4)	−0.06(3)
B	0.1672(4)	0.25	0.8748(4)	1.5(1)	1.9(1)	1.9(1)	0.7(1)	0.1(1)
Sample S5								
O1	0.0209(2)	0.25	0.8676(3)	0.68(6)	0.46(9)	0.6(1)	0.7(1)	−0.1(1)
O2	0.2467(2)	0.25	0.7481(2)	0.73(7)	0.54(7)	0.77(8)	0.74(9)	−0.30(7)
O3	0.2371(2)	0.25	0.0050(2)	0.75(7)	0.55(8)	1.1(1)	0.63(9)	−0.10(6)
O4	0.0101(2)	0.25	0.3834(3)	0.66(6)	0.61(7)	0.83(8)	0.53(7)	−0.12(7)
M1	0.11495(6)	0.25	0.56951(6)	0.52(2)	0.56(2)	0.48(2)	0.52(2)	−0.06(2)
M2	0.10218(9)	0.25	0.19058(8)	0.41(3)	0.33(3)	0.43(3)	0.47(4)	−0.02(3)
B	0.1673(3)	0.25	0.8755(4)	0.60(9)	0.46(9)	0.6(1)	0.7(1)	−0.1(1)
Sample S6								
O1	0.0192(5)	0.25	0.8662(8)	0.7(1)				
O2	0.2478(5)	0.25	0.7484(6)	0.4(1)				
O3	0.2372(6)	0.25	0.0059(6)	0.6(1)				
O4	0.0099(5)	0.25	0.3824(8)	0.59(9)				
M1	0.1150(2)	0.25	0.5696(2)	0.38(5)	0.41(6)	0.29(7)	0.43(7)	−0.01(6)
M2	0.1024(2)	0.25	0.1901(2)	0.50(8)	0.26(8)	0.6(1)	0.6(1)	−0.20(7)
B	0.1672(9)	0.25	0.873(1)	0.8(1)				
Sample S7								
O1	0.0210(2)	0.25	0.8671(3)	0.66(7)	0.37(8)	1.0(1)	0.6(1)	−0.01(8)
O2	0.2470(3)	0.25	0.7470(3)	0.62(8)	0.43(9)	0.9(1)	0.5(1)	0.06(7)
O3	0.2379(3)	0.25	0.0053(3)	0.63(8)	0.33(9)	1.2(1)	0.4(1)	−0.14(7)
O4	0.0095(2)	0.25	0.3843(3)	0.66(7)	0.75(9)	0.8(1)	0.42(9)	0.04(8)
M1	0.11552(7)	0.25	0.56856(7)	0.62(2)	0.57(2)	0.64(3)	0.65(3)	−0.07(2)
M2	0.1025(1)	0.25	0.1904(1)	0.57(3)	0.41(4)	0.66(5)	0.66(4)	0.00(3)
B	0.1663(4)	0.25	0.8740(5)	0.6(1)	0.5(1)	0.7(1)	0.5(1)	0.2(1)

Note: Samples as in Table 2.

* The form of the anisotropic displacement factor is $\exp[-\frac{1}{4}(\beta_{11}h^2a^{*2} + \ldots + 2hla^*c^*\beta_{13})]$. Symmetry restraints for temperature factors: $-\beta_{12} = \beta_{23} = 0$.

tions using a 30 μm objective aperture. The microanalyses were done with the energy-dispersive X-ray detector system EDAX 9100; this instrumental configuration made possible the detailed correlation of chemistry and microstructure.

CHEMICAL RELATIONS

The warwickite samples show wide compositional variation (Tables 1 and 2, Fig. 3). The greatest chemical variations are in Cr_2O_3 (0.00–13.45 wt%; 0.00–1.07 apfu), Fe_2O_3 (22.60–50.63 wt%; 1.66–3.94 apfu), and TiO_2 (0.21–10.15 wt%; 0.02–0.74 apfu). MgO is in the range 25.68–33.20 wt% (3.95–4.82 apfu), and Mn, Ca, Zr, Nb, Al, and Si are minor elements. These variations occur within individual samples and even within individual zoned grains. In most zoned crystals, Cr, Ti, and Mg increase from core to rim, with Fe decreasing dramatically. This compositional variation could be related to the chemical changes induced in the differentiating carbonatite-like magmas by the opaque oxides. These crystallized earlier than or con-

TABLE 5. Selected data from structure refinement of warwickite samples

	S1	S2	S3	S4	S5	S6	S7
B-O1 [Å]	1.358(3)	1.345(4)	1.356(4)	1.358(4)	1.357(4)	1.369(10)	1.347(4)
B-O2 [Å]	1.404(3)	1.413(4)	1.404(4)	1.401(4)	1.402(4)	1.401(12)	1.408(5)
B-O3 [Å]	1.404(3)	1.394(4)	1.383(4)	1.390(4)	1.375(4)	1.390(12)	1.401(5)
⟨B-O⟩ [Å]	1.389	1.384	1.381	1.383	1.378	1.387	1.385
M1-O4 (×1) [Å]	1.970(2)	1.988(2)	1.992(2)	1.991(3)	1.997(3)	2.007(7)	1.991(3)
M1-O4 (×2) [Å]	1.973(1)	1.978(1)	1.984(1)	1.973(1)	1.983(1)	1.983(3)	1.982(2)
M1-O2 (×1) [Å]	2.062(2)	2.058(2)	2.063(2)	2.066(2)	2.071(2)	2.079(5)	2.072(3)
M1-O3 (×2) [Å]	2.133(1)	2.130(1)	2.139(1)	2.131(1)	2.153(1)	2.150(4)	2.142(2)
⟨M1-O⟩ [Å]	2.041	2.044	2.050	2.044	2.057	2.059	2.052
OQE	1.0196	1.0166	1.0160	1.0167	1.0158	1.0158	1.0166
M2-O1 (×2) [Å]	1.992(1)	1.988(1)	1.995(1)	1.987(1)	1.998(1)	1.985(4)	1.998(2)
M2-O4 (×1) [Å]	2.042(2)	2.007(2)	2.003(2)	2.010(3)	1.999(3)	1.997(7)	2.016(3)
M2-O3 (×1) [Å]	2.132(2)	2.139(2)	2.136(2)	2.142(2)	2.142(2)	2.130(6)	2.145(3)
M2-O2 (×2) [Å]	2.146(1)	2.149(1)	2.147(2)	2.145(2)	2.155(2)	2.149(4)	2.149(2)
⟨M2-O⟩ [Å]	2.075	2.070	2.071	2.069	2.075	2.066	2.076
OQE	1.0124	1.0110	1.0108	1.0112	1.0104	1.0114	1.0110

Note: Samples as in Table 2. Bond distances and octahedral quadratic elongation (OQE) as in Robinson et al. (1971).

temporaneously with warwickite, removing Fe from the melt and causing an increase in concentration of Cr and probably Ti (at a slower rate) in the melt. The warwickite samples from the jumillites have very low Cr (Table 1, samples 1–7; Table 2, sample S6).

Two main substitutions occur in the studied warwickites: (1) $Mg^{2+} + Ti^{4+} \rightleftharpoons 2Fe^{3+}$ and (2) $Fe^{3+} \rightleftharpoons Cr^{3+}$. The first substitution characterizes the crystal chemical relations of all the analyzed crystals (Fig. 3a); it seems to prevail in warwickite with low Cr^{3+} content ($Cr^{3+} < 0.2$ apfu) (Figs. 3b and 3c). Substitutions 1 and 2 both occur in samples with Cr^{3+} content in the range $0.20 \leq Cr^{3+} \leq 0.65$ apfu. The substitution mechanism $Mg^{2+} + Ti^{4+} \rightleftharpoons 2Cr^{3+}$ seems to prevail in warwickite with $Cr^{3+} > 0.6$ apfu and $Fe^{3+} < 2.3$ apfu (Fig. 3c).

CRYSTAL CHEMICAL RELATIONS

The seven crystals for which structures were refined cover a wide range of octahedral (M) composition (Table 2). The M cations occupy the M1 and M2 octahedra (Fig. 1), which share edges to form chains of four units M2-M1-M1-M2 rotated at 60° to each other in the (010) plane. The chain interstices are occupied by $(BO_3)^{3-}$ triangles which share the O atoms (O1, O2, O3) with the M1 and M2 octahedra. O4 is shared by octahedra only. The isotropic displacement factors of samples 1–4 are quite high, and this may be ascribed to some positional disorder. In most samples, M1 and M2 have lower values with respect to O and B.

Triangular and tetrahedrally coordinated sites

The B-O1 bond distance is always smaller than B-O2 and B-O3 in Jumilla samples. Previous studies on warwickite related the smaller B-O1 distance to electrostatic bond strength (Venkatakrishnan and Buerger, 1972; Moore and Araki, 1974; Norrestam, 1989). O1 is linked to B and M2, whereas O2 and O3 are linked to B, M1, and M2. Furthermore, the octahedral composition seems to affect mainly B-O1 and B-O3 individual bond distances (1.345 Å ≤ B-O1 ≤ 1.369 Å; 1.375 Å ≤ B-O3 ≤ 1.404 Å), whereas B-O2 remains almost unchanged.

Si in warwickite has been assigned to the tetrahedral sites by analogy with cuspidine. By substituting a $(Si_2O_7)^{6-}$ group for a $(B_2O_6)^{6-}$ group, the sequence . . . B □ B □ B□ . . . along the [010] direction is changed to the sequence . . . Si O Si □ Si O Si . . . as for cuspidine (Merlino and Perchiazzi, 1988). It was not possible to determine if the $(Si_2O_7)^{6-}$ groups are randomly distributed or if they form cuspidine-type domains within warwickite, as the Si content is too low.

Octahedrally coordinated sites

The mean atomic number at each cation site, calculated from the electron probe analysis, agrees quite well with

TABLE 7. Mean atomic number for octahedral sites, determined by structure refinement and microprobe analysis for the studied warwickite samples

	S1	S2	S3	S4	S5	S6	S7
M1 Xref	10.28(3)	10.15(3)	10.06(3)	9.82(4)	10.00(4)	9.50(10)	10.13(5)
M2 Xref	7.92(2)	7.27(3)	7.17(3)	7.14(3)	7.40(4)	7.36(9)	7.43(4)
M1 + M2 Xref*	36.40	34.84	34.46	33.92	34.80	33.72	35.12
M1 + M2 EPMA**	36.45	34.95	34.50	34.08	35.02	34.44	35.29

Note: Samples as in Table 2; Xref: X-ray refinement; EPMA: electron microprobe analysis ($Z = 4$).
* 2 × (M2 + M1).
** Sum of octahedral cation electrons.

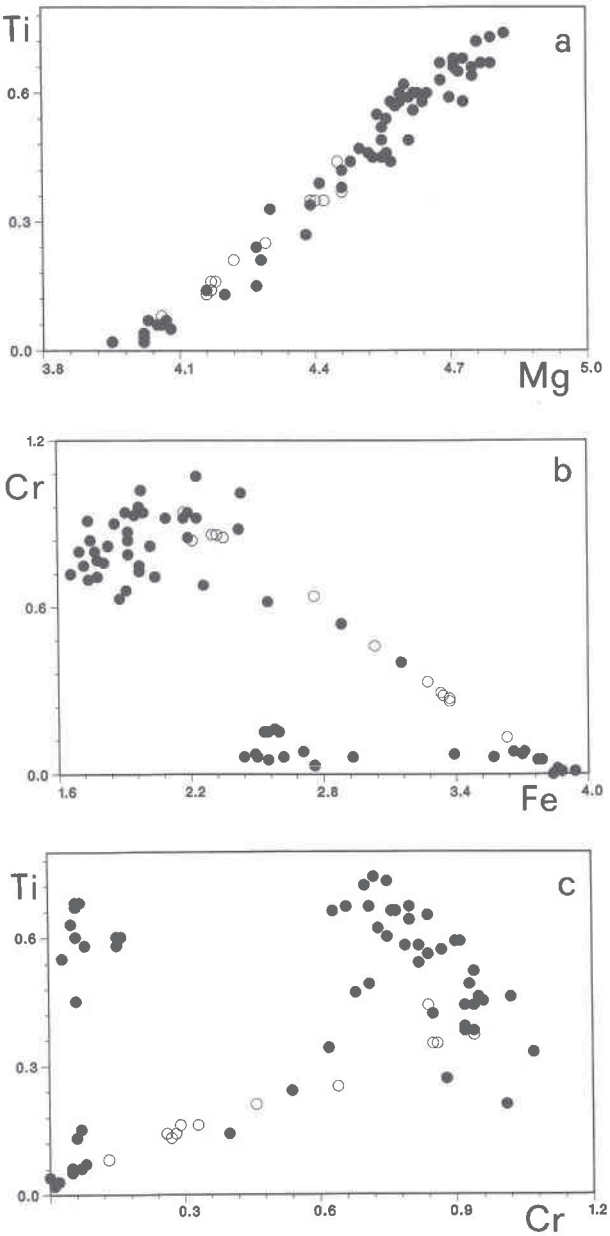

Fig. 3. Ti vs. Mg (**a**), Cr vs. Fe (**b**); Ti vs. Cr (**c**) (atoms pfu). Open circles refer to the profile of a zoned crystal (sample M6). Filled circles refer to unzoned warwickite crystals and to the mean value of zoned warwickite crystals.

that from the X-ray refinement (Table 7). The agreement is not as good for sample S6, perhaps because the chemical analysis is the average of determinations on several crystals from the same rock sample. The site refinements indicate that M1 is enriched in (Fe,Cr) relative to M2, in agreement with the results of Norrestam (1989).

The octahedral distortion OQE (Robinson et al., 1971) was used to describe the deformation of octahedra. The M1 octahedra are smaller and more distorted than the

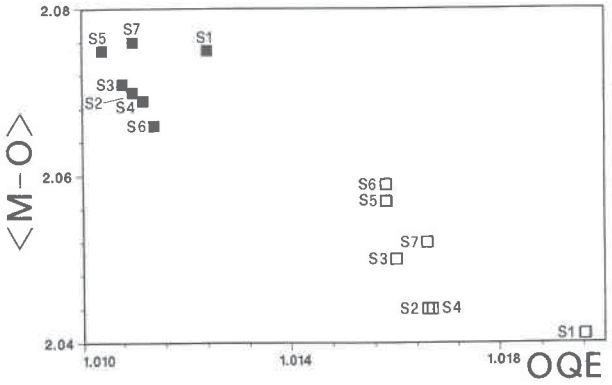

Fig. 4. Mean ⟨M-O⟩ [Å] vs. OQE for M1 (open squares) and M2 (filled squares) octahedra.

M2 octahedra (M1-O = 2.041–2.059 Å, M2-O = 2.066–2.076 Å, OQE_{M1} = 1.0160–1.0196, OQE_{M2} = 1.0104–1.0124; Table 5).

With increasing ⟨M1-O⟩ and ⟨M2-O⟩ distances, the distortion parameter decreases (Fig. 4). Furthermore, in Fe-rich warwickite (sample S1), the average distance is smaller and the distortion is higher than in Mg-, Ti-rich warwickite.

The individual bond distances M-O1 and M-O4 are smaller than the mean ⟨M-O⟩ distance at both sites. The increase in Ti in the Jumilla warwickite samples causes the decrease in M2-O4 (r = −0.898, Fig. 5) and a corresponding increase in the M1-O4 distance. Thus, it seems that the occurrence of Ti at M2 induces the substitution of Fe for Mg at M1. Moore and Araki (1974) suggest that Ti in Ti-rich warwickite preferentially substitutes at M1.

Microstructures

Although the low R values obtained for structure refinements support a well-ordered atomic arrangement, many crystals examined during the preliminary investigations showed structural disorder and chemical zoning.

Bovin et al. (1981), in a study of structural defects in

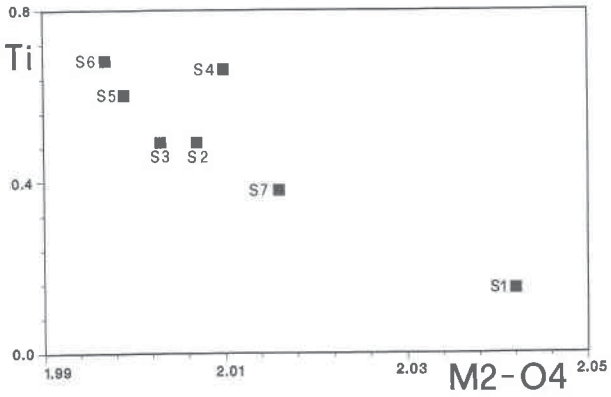

Fig. 5. Ti (atoms pfu) content vs. M2-O4 individual bond distance [Å].

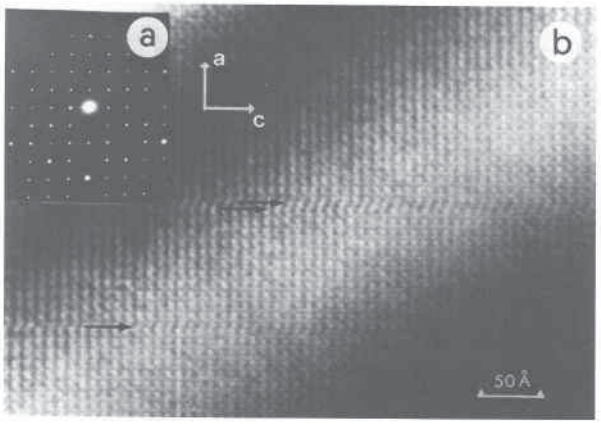

Fig. 6. Selected area electron diffraction pattern (**a**) and electron micrograph (**b**) of a warwickite crystal oriented with **b** parallel to the electron beam. Distances between the white spots correspond to the cell parameters *a* and *c*. One isolated defect and one pair of defects are marked by arrows.

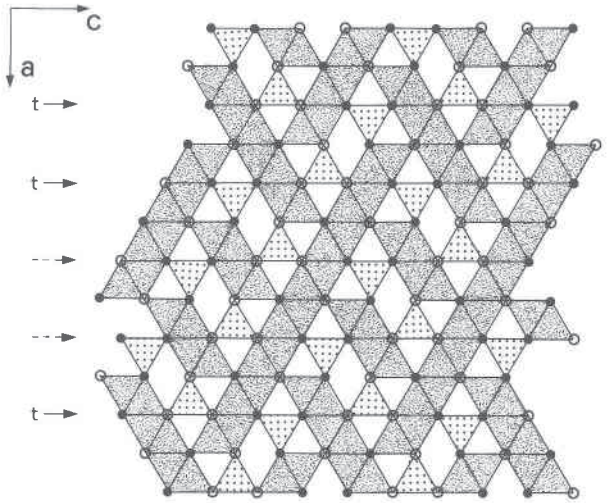

Fig. 7. Schematic representation of the pair of defects shown in Figure 6. The structure of warwickite is viewed down the **b** axis. Black and open circles are as in Figure 1. The omission of two consecutive twin operations, t, generates chains eight octahedra wide, linked by chains of two octahedra.

oxyborates with the general formula $^{[6]}M_3{}^{[3]}BO_5$, described the structures as a sequence of *n* octahedral layers (n = 2, 4, 6 for ludwigite, orthopinakiolite, and takéuchiite, respectively) between slip (s) or twin (t) planes. The structure of warwickite may thus be indicated as . . . 2t2t . . . , in which the twin axis (or rotation axis) is perpendicular to (100) and passes through the center of a B triangle. The most common structural defects of the warwcikite samples examined occur in (100), changing the sequence from the type . . . 2t2t . . . to the type . . . 2t22t . . . . Figure 6a shows a typical selected area electron diffraction (SAED) pattern of warwickite crystals oriented with **b** parallel to the electron beam. It is characterized by well-defined spots, indicating a low proportion of defects. The corresponding high-resolution electron micrograph is shown in Figure 6b, in which the periods of white dots define the **a** and **c** cell translations. The defects observed in a number of crystals are of the same kind as illustrated in Figure 6b and occur randomly in the sequence. They are produced by the shift of a row of white dots (½**a** + ¼**c**) with respect to an adjacent row of the undisturbed structure. In places, this defect is repeated twice (Fig. 6b), generating a sequence of the type . . . 2t222t . . . . As shown in Figure 7, this sequence gives rise to chains eight octahedra wide, linked by chains of two octahedra that retain their original orientation. It is not possible to discern differences in the topologies of the M1 and M2 polyhedra in the new arrangement. Apparently the appearance of the structural defects is not controlled by the chemical composition (as revealed by electron microprobe analyses made on different zones of the same crystal); it is probable that it is induced in the growing crystals by some impurity (Bovin et al., 1981).

Conclusions

The warwickite samples from Jumilla are chemically variable and are characterized by high Fe and Cr contents. The occurrence of Cr-rich varieties is unique for the warwickite family and is also rare in the natural oxyborates (Hawthorne, 1986). It is reasonable to hypothesize the existence of natural Cr and Fe end-members of the warwickite family. The warwickite samples studied show the following main substitutions: $Mg^{2+} + Ti^{4+} \rightleftharpoons 2Fe^{3+}$ and $Fe^{3+} \rightleftharpoons Cr^{3+}$. Coupled substitutions occur at both M1 and M2 octahedral sites; Fe and Cr are concentrated in M1, whereas Mg and Ti dominate at M2. Presumably the occurrence of Ti at M2 is locally coupled to Mg at M1.

Many crystals are chemically zoned and show planar (100) defects, causing variations in the octahedral chain lengths. In oxyborates having the general formula $^{[6]}M_3{}^{[3]}BO_5$, different structures are generated through the regular repetition of similar structural defects (Bovin et al., 1981). The possibility of generating comparable structures through the repetition of such defects also seems reasonable for warwickite. These defects are not related to variation in pressure and temperature conditions of crystallization, as the analyzed crystals come from the same veinlet and they seem to be independent of the chemical composition for the crystals. Probably these defects are induced in the growing crystals by some impurity.

Acknowledgments

We wish to thank S. Merlino of Pisa University and G. Venturelli of Parma University for useful discussion and critical reading of the manuscript. Thanks are also due to P.B. Moore and F.C. Hawthorne for their helpful suggestions and stylistic improvements. The Centro Interdipartimentale di Calcolo (CICAIA) and Centro Grandi Strumenti (CGS) of Modena University are acknowledged for their technical support and the CNR for the use of the ARL-SEMQ electron microprobe at the Istituto di Mineralogia e Petrografia, Università di Modena. Financial support

was given by Ministero della Università della Ricerca Scientifica e Tecnologica and by CNR (grant 89.00360.05).

References cited

Albee, A.L., and Ray, L. (1970) Correction factors for electron microanalysis of silicates, oxides, carbonates, phosphates and sulphates. Analytical Chemistry, 42, 1408–1414.

Bovin, J.-O., O'Keeffe, M., and O'Keefe, M.A. (1981) Electron microscopy of oxyborates. I. Defect structures in the minerals pinakiolite, ludwigite, orthopinakiolite and takéuchiite. Acta Crystallographica, A37, 28–35.

Einstein, J.R. (1974) Analysis of intensity measurements of Bragg reflections with a single crystal equatorial plane diffractometer. Journal of Applied Crystallography, 7, 331–344.

Fuster, J.M., Gastesi, P., Sagrado, J., and Fermoso, M.L. (1967) Las rocas lamproiticas del SE de España. Estudios Geologicos, 23, 35–69.

Hawthorne, F.C. (1986) Structural hierarchy in $^{VI}M_x^{III}T_y\Phi_2$ minerals. Canadian Mineralogist, 24, 625–642.

International Tables for X-ray Crystallography (1974) Kinoch Press, Birmingham.

Malinko, S.V., Yamnova, N.A., Pushcharowskii, D.Y., Lisitsin, A.E., Rudnev, V.V., and Yurkina, K.V. (1986) Iron-rich warwickite from the Taiga ore deposit (southern Yakutia). Zapiski Vsesoyuznogo Mineralogicheskogo Obshchestva, 115, 713–719 (in Russian).

Merlino, S., and Perchiazzi, N. (1988) Modular mineralogy in the cuspidine group of minerals. Canadian Mineralogist, 26, 933–943.

Moore, P.B., and Araki, T. (1974) Pinakiolite, $Mg_2Mn^{3+}O_2[BO_3]$; warwickite, $Mg(Mg_{0.5}Ti_{0.5})\ O[BO_3]$; wightmanite, $Mg_5(O)(OH)_5[BO_3]\cdot nH_2O$: Crystal chemistry of complex 3 Å wallpaper structures. American Mineralogist, 59, 985–1004.

Nobel, F.A., Andriessen, P.A.M., Habeda, E.H., Priem, H.N.A., and Rondeel, H.E. (1981) Isotopic dating of the post-Alpine neogene volcanism in the Betic Cordilleras, Southern Spain. Geologische Mijnbouw, 60, 209–214.

Norrestam, R. (1989) Structural investigation of two synthetic warwickites: Undistorted orthorhombic $MgScOBO_3$ and distorted monoclinic $Mg_{0.76}Mn_{1.24}OBO_3$. Zeitschrift für Kristallographie, 189, 1–11.

North, A.C.T., Phillips, D.C., and Mathews, F.S. (1968) A semi-empirical method of absorption correction. Acta Crystallographica, A24, 351–359.

Osann, A. (1906) Über einige Alkaligesteine aus Spanien. H. Rosenbusch Fortschrift, Stuttgart, 283–301.

Robinson, K., Gibbs, G.V., and Ribbe, P.H. (1971) Quadratic elongation: A quantitative measure of distortion in coordination polyhedra. Science, 172, 567–570.

Sheldrick, G.M. (1976) SHELX-76. Programme for crystal structure determination. University of Cambridge, Cambridge, England.

Takéuchi, Y., Watanabé, T., and Ito, T. (1950) The crystal structures of warwickite, ludwigite and pinakiolite. Acta Crystallographica, 3, 98–107.

Venkatakrishnan, V., and Buerger, M.J. (1972) The crystal structure of $FeCoOBO_3$. Zeitschrift für Kristallographie, 135, 321–338.

Venturelli, G., Capedri, S., Di Battistini, G., Crawford, A., Kogarko, L.N., and Celestini, S. (1984) The ultrapotassic rocks from southeastern Spain. Lithos, 17, 37–54.

Venturelli, G., Capedri, S., Barbieri, M., Toscani, L., Salvioli Mariani, E., and Zerbi, M. (1991) The Jumilla lamproite revisited: A petrological oddity. European Journal of Mineralogy, 3, 123–145.

Ziebold, T.O., and Ogilvie, R.E. (1964) An empirical method for electron microanalysis. Analytical Chemistry, 36, 322–327.

Manuscript received August 10, 1990
Manuscript accepted April 6, 1991